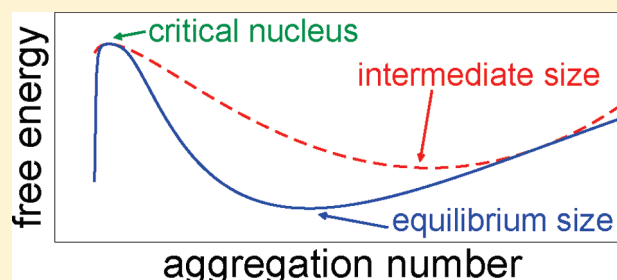# Kinetics of Surfactant Micellization: A Free Energy Approach

Radina Hadgiivanova,[†] Haim Diamant,[*,†] and David Andelman[‡]

[†]Raymond and Beverly Sackler School of Chemistry and [‡]Raymond and Beverly Sackler School of Physics and Astronomy, Tel Aviv University, Tel Aviv 69978, Israel

ABSTRACT: We present a new theoretical approach to the kinetics of micelle formation in surfactant solutions, in which the various stages of aggregation are treated as constrained paths on a single free-energy landscape. Three stages of well-separated time scales are distinguished. The first and longest stage involves homogeneous nucleation of micelles, for which we derive the size of the critical nuclei, their concentration, and the nucleation rate. Subsequently, a much faster growth stage takes place, which is found to be diffusion-limited for surfactant concentrations slightly above the critical micellar concentration (cmc) and either diffusion-limited or kinetically limited for higher concentrations. The time evolution of the growth is derived for both cases. At the end of the growth stage, the micelle size may be either larger or smaller than its equilibrium value, depending on concentration. A final stage of equilibration follows, during which the micelles relax to their equilibrium size through fission or fusion. Both cases of fixed surfactant concentration (closed system) and contact with a reservoir of surfactant monomers (open system) are addressed and found to exhibit very different kinetics. In particular, we find that micelle formation in an open system should be kinetically suppressed over macroscopic times and involve two stages of micelle nucleation rather than one.

INTRODUCTION

Self-assembly of amphiphilic molecules into mesoscopic aggregates (micelles) in solution is a common and thoroughly investigated phenomenon.[1] Dynamic aspects of this process have been extensively studied as well.[2] The techniques applied in such experiments and the interpretation of their results have used the framework of reaction kinetics, where each aggregate size is treated as a distinct chemical species and changes in size and population are treated as chemical reactions (ref 2, chapter 3). Two well-separated time scales are identified in experiments.[3] The shorter of the two, denoted τ_1 (typically $\sim 10^{-5} - 10^{-4}$ s), corresponds to the exchange of a single molecule between a micelle and the monomeric solution; during this time scale, the number of micelles remains essentially fixed. The second time scale, τ_2 (which widely varies and may be, e.g., about $\sim 10^{-2}$ s), is associated with overcoming the barrier to the formation or disintegration of an entire micelle. The total activation time for such a process is $m\tau_2$, where m is the number of molecules in a micelle. During this longer time scale, the number of micelles changes.

The first and still prevalent theory of micellar kinetics by Aniansson and Wall[4] is based on these observations. It casts the micellization process in the form of reaction kinetics with two well-separated time scales, whereby micelles form and disintegrate through a series of single monomer exchange reactions. While various extensions to the Aniansson—Wall theory have been presented over the years,[5−13] only a few alternative approaches have been suggested. In ref 14, the interesting possibility that micellization may behave as a bistable autocatalytic reaction was explored. An idealized (one-dimensional) nucleation model for linear aggregates was suggested in ref 15.

An important alternative approach to study micellization kinetics has been the use of computer simulations.[16−23] In the case of micellization of amphiphilic block copolymers, more progress has been achieved (ref 2, chapter 4; refs 24−32). The kinetics of such polymeric micelles, however, usually depends on qualitatively different effects, in particular, the high entropy barrier for polymer penetration into a micelle.

In the current work, we present a new approach to the kinetics of surfactant micellization, which is based on a free-energy formalism. A similar strategy was previously applied to the kinetics of surfactant adsorption at interfaces.[33,34] This approach has two main advantages. The first is that it provides a more unified description of the kinetics. Rather than considering different stages as separate processes ("reactions"), they can all be cast as constrained pathways on a single free-energy landscape. Considering different processes on the same footing allows, for example, easier identification of rate-limiting stages such as diffusion-limited or kinetically limited ones.[34] The second advantage of such a formalism is that it can be relatively easily extended to more complex situations, such as ionic solutions or surfactant mixtures.[35] On the other hand, the shortcoming of the model is that it is phenomenological, following coarse-grained thermodynamic variables rather than those characterizing single molecules and aggregates. It is probably not appropriate for large polymeric micelles, where intrachain degrees of freedom play an important role and a more detailed

description of molecules and aggregates is required.[24,27,28] We shall focus here, therefore, on the micellization of short-chain surfactants.

Another consequence of the coarse-grained modeling is that the derivation for the kinetics of micellization bears similarities to the kinetics of first-order phase transitions, an analogy that was previously invoked.[15,27] However, unlike macroscopic phase separation, micellization is restricted to finite-size aggregates, resulting, for example, in growth laws that are not scale-free.

In the next section, we present the free-energy formalism and its implications for the process of micelle formation. As in previous theories, we subsequently separate the kinetics into stages of disparate time scales, during each of which a different set of constraints is imposed. We discuss separately the kinetics of closed and open systems. A closed system contains a fixed number of surfactant molecules. In an open system, the surfactant solution is in contact with a large reservoir, which is at thermodynamic equilibrium. Whereas in equilibrium this distinction is usually immaterial, the kinetics of the two cases are found to be strikingly different. While reading through the various stages of micellization, it may be helpful to refer to the two schematic diagrams provided at the end of the article (Figures 13 and 14 for closed and open systems, respectively). The first stage that we address is the nucleation of micelles. Subsequently, we describe the growth of the micellar nuclei as they absorb additional monomers from the surrounding solution. Both options of kinetically limited and diffusion-limited growth are studied. In addition, the possible role of long-distance diffusive transport is examined. We then consider the final relaxation toward equilibrium. Finally, we summarize the conclusions and discuss the experimental implications of our analysis, as well as its limits of validity.

■ MODEL

The model is based on a simple free-energy functional, which has been recently introduced to study metastability issues of micellization.[36] Apart from the temperature T, the free energy depends on three thermodynamic degrees of freedom, which we take to be the total volume fraction of surfactant in the solution, Φ, the volume fraction of surfactant monomers, Φ_1, and the number of molecules in a micelle (aggregation number), m. Despite the simplified two-state (monomer–aggregate) description, polydispersity can be accounted for as fluctuations of the variable m.[37] (This, however, restricts the validity of the model to compact micelles whose size distribution is narrow.[1]) All energies hereafter are given in units of the thermal energy, $k_B T$.

The free energy has contributions from the entropy of mixing and from the interactions among surfactant molecules. The former is obtained from a coarse-grained lattice scheme (Flory–Huggins model), in which a water molecule occupies a single lattice cell of volume a^3 and a surfactant molecule is larger and occupies n such cells. The interactions in the solution are represented by a single phenomenological function, $u(m)$, which is assumed to capture all of the molecular contributions to the free energy of transferring a surfactant molecule from the solution into an aggregate of size m. The resulting Helmholtz free-energy density (per lattice site) is[36]

$$F(\Phi, \Phi_1, m) = \frac{\Phi_1}{n} \ln \Phi_1 + \frac{\Phi_m}{nm}[\ln \Phi_m - mu(m)] + (1-\Phi)\ln(1-\Phi) \quad (1)$$

where $\Phi_m = \Phi - \Phi_1$ is the volume fraction of micelles and $1 - \Phi$ is the volume fraction of water. At equilibrium, the solution is spatially uniform and characterized by those single mean values of the variables, which minimize the free energy under the appropriate constraints. For a closed system, F is minimized with respect to Φ_1 and m for a given Φ. For an open system, one should minimize $F - \mu\Phi$ with respect to Φ, Φ_1, and m for a given surfactant chemical potential μ. Out of equilibrium, the values of variables, such as Φ, Φ_1, and m, may be position-dependent, and the total free energy is given by spatial integration of the local free-energy density. (We neglect here surface tension (gradient) terms associated with boundaries between such spatial domains.)

The specific choice of the interaction function $u(m)$ is not crucial so long as it has a maximum at a finite m to ensure the stability of finite-size micelles. To provide numerical examples, and following previous works,[36,38] we use a simple three-parameter function

$$u(m) = u_0 - \sigma m^{-1/3} - \kappa m^{2/3} \quad (2)$$

The first term in eq 2 represents a micelle-size-independent free-energy gain in increasing m, the second is a surface energy penalty, and the third is responsible for stabilizing a finite-size aggregate. (For a more detailed discussion of these terms and the restricted ranges of relevant values for u_0, σ, and κ, see ref 36.)

Despite its simplicity, eq 1 defines a rather rich free-energy landscape over a three-dimensional space of macrostates, parametrized by the axes (Φ, Φ_1, m). We are going to treat the kinetics of micellization as time-dependent paths along this landscape, and it is beneficial, therefore, to first recall its key features,[36] demonstrated in Figure 1. For any given Φ and along the Φ_1 axis, F always has a single minimum at $\Phi_1 = \Phi_1^*(m, \Phi)$ for all values of m. This value of monomer volume fraction as a function of aggregation number and total volume fraction is found by solving the equation

$$\Phi_1 = \Phi_1^*(m, \Phi): \quad (\Phi_1)^m e^{mu(m)+m-1} = \Phi - \Phi_1 \quad (3)$$

Along the m axis, however, F becomes nonconvex when Φ exceeds a certain volume fraction, φ_1, with two minima at $m = 1$ and $m^*(\Phi_1, \Phi)$ and a maximum in between at $m = m_{nuc}(\Phi_1, \Phi)$ (see Figure 1A and B). The extrema satisfy the equation

$$m = m^*, m_{nuc}: \quad m^2 = -\ln(\Phi - \Phi_1)/u'(m) \quad (4)$$

where $u' = du/dm$. Combining eqs 3 and 4, we can find m and Φ_1 at the extrema for a given Φ according to

$$m = m^*, m_{nuc}: \quad m^2 = -\ln[\Phi - e^{-u(m)-mu'(m)-1+1/m}]/u'(m) \quad (5)$$

$$\Phi_1^* = e^{-u(m)-mu'(m)-1+1/m} \quad (6)$$

Above a larger volume fraction, $\varphi_2 > \varphi_1$ (Figure 1C), the micellar state with $\Phi > \varphi_2$, $m = m^*$, and $\Phi_1 = \Phi_1^*(m^*, \Phi)$, though still metastable, may become appreciably occupied, giving rise to premicellar aggregates.[36] Above yet another volume fraction, $\varphi_3 > \varphi_2$ (Figure 1D), the micellar state for $\Phi > \varphi_3$ becomes the global minimum of F. It is this point, analogous to the binodal line in phase separation, which corresponds to the commonly defined cmc,[36] that is, $cmc = c_3 = \varphi_3/(na^3)$. We shall focus in the current
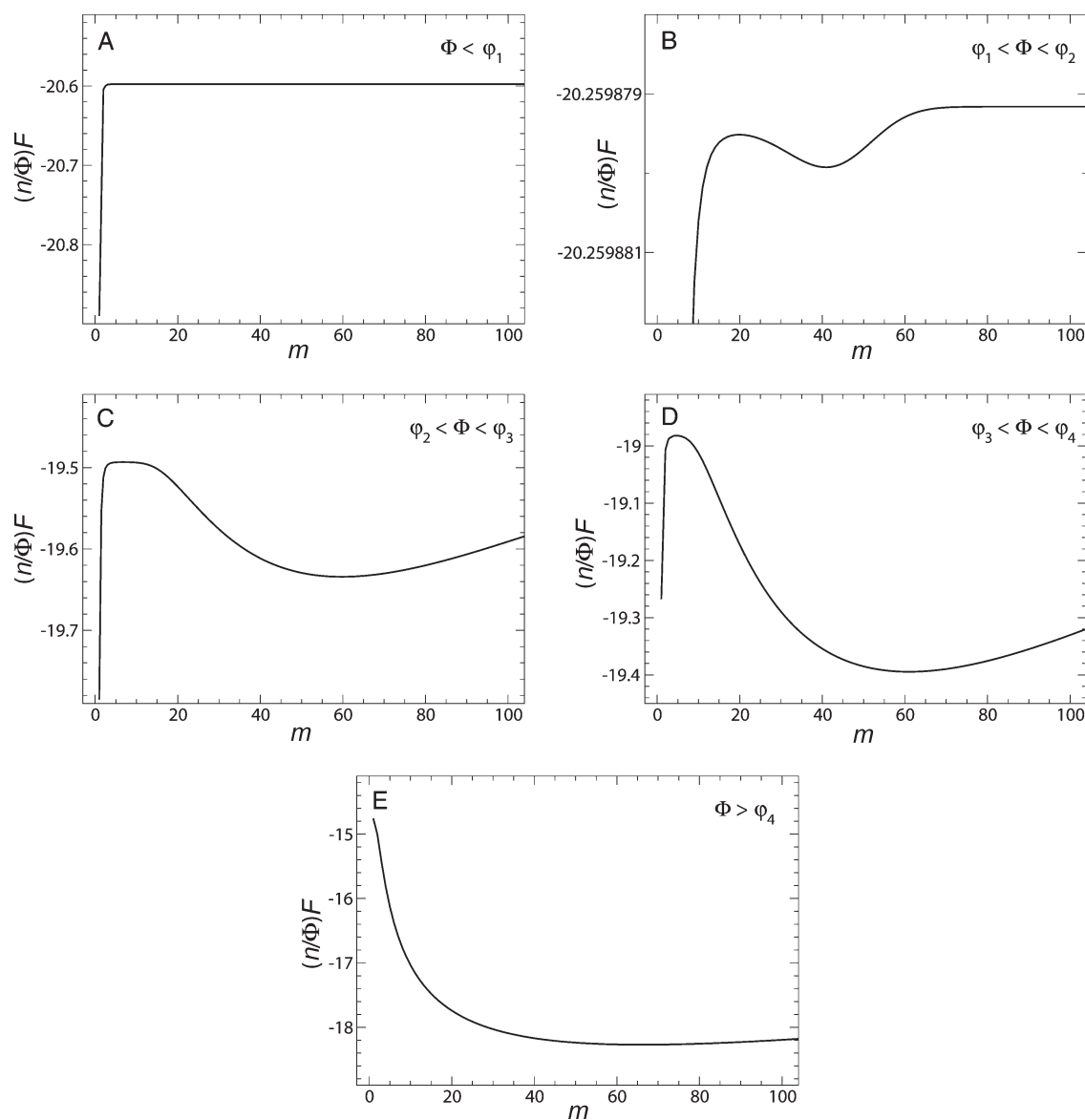
Figure 1. Cuts of the free-energy landscape (per surfactant molecule, in units of $k_B T$) as a function of aggregation number along the $\Phi_1^*(m)$ line for the surfactant parameters of Table 1 and increasing surfactant volume fraction, Φ: (A) $\Phi = 5 \times 10^{-4} < \varphi_1$; (B) $\varphi_1 < \Phi = 7 \times 10^{-4} < \varphi_2$; (C) $\varphi_2 < \Phi = 1.5 \times 10^{-3} < \varphi_3 = \varphi_{cmc}$; (D) $\varphi_3 < \Phi = 2.5 \times 10^{-3} < \varphi_4$; and (E) $\Phi = 0.11 > \varphi_4$.

work on the ordinary micellization region, $\Phi > \varphi_3 = \varphi_{cmc}$, where micelles are stable at equilibrium. It should be kept in mind, however, that in this region, the monomeric and micellar states are separated by a free-energy barrier in the form of a saddle point of F, $F_{nuc}(\Phi) = F[\Phi,\Phi_1^*(m_{nuc},\Phi),m_{nuc}]$. The barrier may be high, leading to the measurement of an apparent *cmc*, which is higher than the equilibrium one, $\varphi_3 = \varphi_{cmc}$.[13] Finally, above a certain higher volume fraction, $\varphi_4 > \varphi_3$, the barrier disappears, and the micellar state for $\Phi > \varphi_4$ remains the sole minimum of F, as seen in Figure 1E. (This work is restricted to the isotropic micellar phase of surfactant solutions; at higher concentrations, other phases and mesophases appear.[1]) The point $\Phi = \varphi_4$ is the analogue of the spinodal line in macroscopic phase separation. As already mentioned in the Introduction, despite the analogy with phase separation, it should be borne in mind that micellization is essentially different in that it involves finite-size aggregates and smooth crossovers rather than macroscopic phases and sharp transitions.

The initial and final states of the micellization kinetics are defined as follows. At $t = 0$, the system is in the monomeric state, $(\Phi_1 = \Phi, m = 1)$, whereas its equilibrium state is the micellar one. In a closed system, this is done by setting the surfactant volume fraction above the *cmc*, $\Phi > \varphi_3$ (using, for example, the temperature jump or stopped flow techniques[2]). In an open system, the initial condition corresponds to opening a diffusive contact with a bulk reservoir, whose surfactant volume fraction Φ_b is above the *cmc*, $\Phi_b > \varphi_3$. The reservoir is assumed to have already reached the equilibrium micellar state. At $t \to \infty$, the system reaches the global minimum of the free energy, $[\Phi,\Phi_1^*(m^*,\Phi),m^*(\Phi)]$ in the closed case and $[\Phi_b,\Phi_1^*(m^*,\Phi_b), m^*(\Phi_b)]$ in the open one. In what follows, we consider the kinetic pathway that the system takes between these initial and final states. Assuming separation of time scales, we shall divide the temporal path into separate stages. Note that the various time scales are derived from the free-energy functional and a single

Table 1. Parameters of the Exemplary Surfactant and the Resulting Boundaries of the Micellar Region

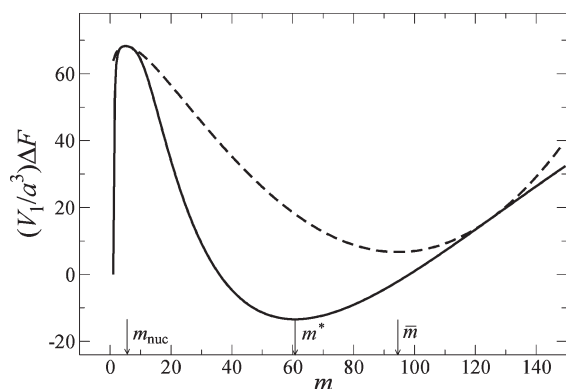| n	u_0	σ	κ	$\varphi_3 = \varphi_{cmc}$	φ_4
13	10	11	0.08	2.03×10^{-3}	0.106

Figure 2. Cuts of the free-energy landscape (relative to the monomeric state, per micelle, in units of k_BT) as a function of aggregation number for the surfactant parameters of Table 1 and $\Phi = 1.1\varphi_3$. The two curves correspond to two different constraints, relaxation of the monomer volume fraction for the given aggregation number (solid) and fixed concentration of micelles (dashed). Indicated by arrows are the sizes of the critical nucleus (m_{nuc}), the intermediate aggregate at the end of the growth stage ($\bar{m}$), and the equilibrium micelle (m^*). A closed system is assumed. V_1 is the volume of the solution per micelle at equilibrium.

molecular time, τ_0, thus enabling comparison of different stages and processes.

Throughout the following sections, we demonstrate the results using a single exemplary surfactant, whose parameters are listed in Table 1. This allows comparison with refs 36 and 37, where the behavior of the same exemplary surfactant for $\Phi < \varphi_3 = \varphi_{cmc}$ was presented.

Figure 2 shows two cuts through the free-energy landscape as a function of aggregation number for the exemplary surfactant in a closed system at a total surfactant volume fraction slightly larger than $\varphi_3 = \varphi_{cmc}$. Along the first cut (solid line), the monomer volume fraction is assumed to be at quasi-equilibrium, $\Phi_1 = \Phi_1^*(m)$. Thus, the minimum of this curve corresponds to the global minimum — the equilibrium aggregation number. Along the other cut (dashed curve), which is relevant to the next two sections, we constrain the concentration of micelles to remain at its nucleation value.

■ MICELLAR NUCLEATION

Closed System. Let us set the total volume fraction at $t = 0$ to some value, $\Phi > \varphi_3 = \varphi_{cmc}$, and assume that the value (apart from a short initial period of homogenization, which is ignored) remains fixed and uniform throughout the micellization process. The first stage to consider is the ascent of the free energy from the initial metastable state, $(\Phi, \Phi_1 = \Phi, m = 1)$, to the saddle point $[\Phi, \Phi_1 = \Phi_1^*(m_{nuc}), m = m_{nuc}]$, that is, the formation of the critical nuclei. This activated process is assumed to be much slower than diffusion. Hence, Φ_1 can be taken during this stage as spatially uniform and equal to the value that minimizes the free energy for the given Φ and $m(t)$. Thus, as $m(t)$ increases from 1 to the critical nucleus size m_{nuc}, the system proceeds along the path that satisfies the constraints $\Phi = $ const and $\Phi_1 = \Phi_1^*[m(t), \Phi]$.

A similarly constrained path was studied in detail in ref 37 to obtain the lifetime of metastable micelles in the region $\varphi_2 < \Phi < \varphi_3$ using Kramers' theory. Such a rigorous calculation, unfortunately, cannot be repeated here because the metastable monomeric state is actually not a local minimum of F but just the edge, at $m = 1$, of the range of allowed aggregation numbers (see Figure 1D). Nevertheless, as demonstrated in ref 37, the nucleation time (dissociation time in ref 37) and its concentration dependence are primarily determined by the height of the free-energy barrier.

The free-energy barrier corresponds to the nucleation of a single micelle. Our model, however, considers macrostates of a solution containing many micelles and monomers. To switch between these two descriptions, we introduce a subsystem volume, V_1, which contains (on average) a single nucleus. The volume fraction of critical nuclei, their concentration, and the volume per nucleus are readily given for closed systems by

$$
\begin{aligned}
\Phi_{nuc}(\Phi) &= \Phi - \Phi_1^*[m_{nuc}(\Phi), \Phi] \\
c_{nuc}(\Phi) &= \Phi_{nuc}(\Phi)/[na^3 m_{nuc}(\Phi)] \\
V_1(\Phi) &= c_{nuc}^{-1} = \frac{na^3 m_{nuc}(\Phi)}{\Phi - \Phi_1^*[m_{nuc}(\Phi), \Phi]}
\end{aligned}
\tag{7}
$$

where $m_{nuc}(\Phi)$ and $\Phi_1^*(\Phi)$ are given by eqs 5 and 6. Since Φ_{nuc} is very small, V_1 is much larger than the molecular volume, and our coarse-grained approach is indeed applicable. Note the distinction between the nuclei concentration c_{nuc} and their volume fraction Φ_{nuc}. Since the micelle size m is a variable, constraining c_{nuc} does not imply a fixed Φ_{nuc}. This will be important in the next sections when we impose a constraint on the number of nuclei. The nucleation barrier and nucleation time scale are given for closed systems by

$$
\begin{aligned}
\Delta F_{nuc}(\Phi) &= \frac{V_1(\Phi)}{a^3}\{F[\Phi, \Phi_1^*(m_{nuc}, \Phi), m_{nuc}] - F_1(\Phi)\} \\
\tau_{nuc}(\Phi) &\simeq \tau_0 e^{\Delta F_{nuc}(\Phi)}
\end{aligned}
\tag{8}
$$

where τ_0 is a molecular time scale and F_1 is the free energy of the monomeric state. It should be mentioned that our formalism artificially distinguishes between monomers and aggregates of size $m = 1$. As in the previous works,[36,37] this artifact has an insignificant effect on the results. We calculate here the free energy of the $m = 1$ state as $F_1(\Phi) = F[\Phi, \Phi_1^*(1, \Phi), 1]$.

Various features of the nucleation stage can be calculated from eqs 1–8, as demonstrated in Figures 3–5. The concentration of critical nuclei (Figure 3A) sharply increases with surfactant volume fraction as Φ is increased above $\varphi_3 = \varphi_{cmc}$. The size of the critical nucleus (Figure 4A) decreases with Φ until it practically vanishes as Φ approaches φ_4. The height of the nucleation barrier (Figure 5) decreases as well with Φ, leading to a sharp decrease in the nucleation time scale (Figure 5, inset). To get an estimate of the actual nucleation time scales, we may take $\tau_0 \approx 10^{-8}$ s, which is the time that it takes a molecule with a diffusion coefficient of $\sim 10^{-6}$ cm^2 s^{-1} to be displaced by ~ 1 nm. For the example presented in Figure 5, τ_{nuc} is extremely large close to φ_3 but drops to ~ 1 s for $\Phi \simeq 2\varphi_3$.

Open System. When the system is placed in contact with a large reservoir of volume fraction Φ_b, $\Phi_b > \varphi_3 = \varphi_{cmc}$, monomers will first diffuse in, until the monomeric concentrations are balanced. We shall assume that micellar diffusion from the
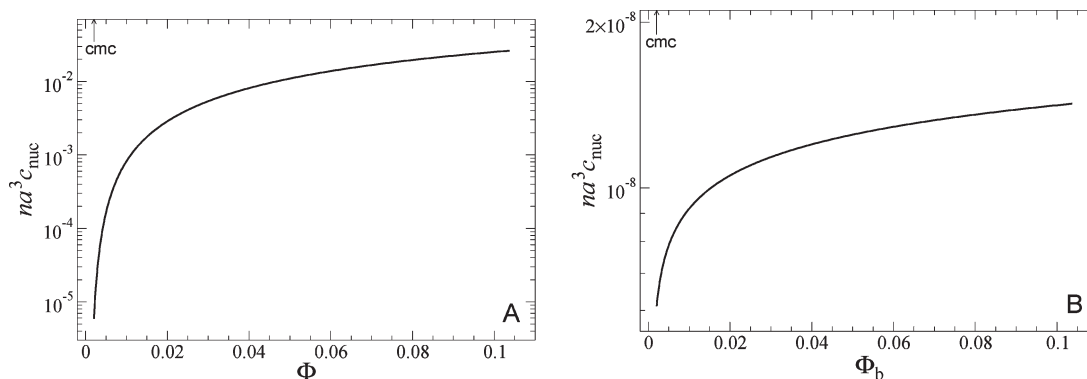
Figure 3. Concentration of critical nuclei (normalized by the molecular volume) as a function of surfactant volume fraction in the range between $\varphi_3 = \varphi_{cmc} \simeq 2 \times 10^{-3}$ and φ_4 for closed (A) and open (B) systems. Parameters are given in Table 1.
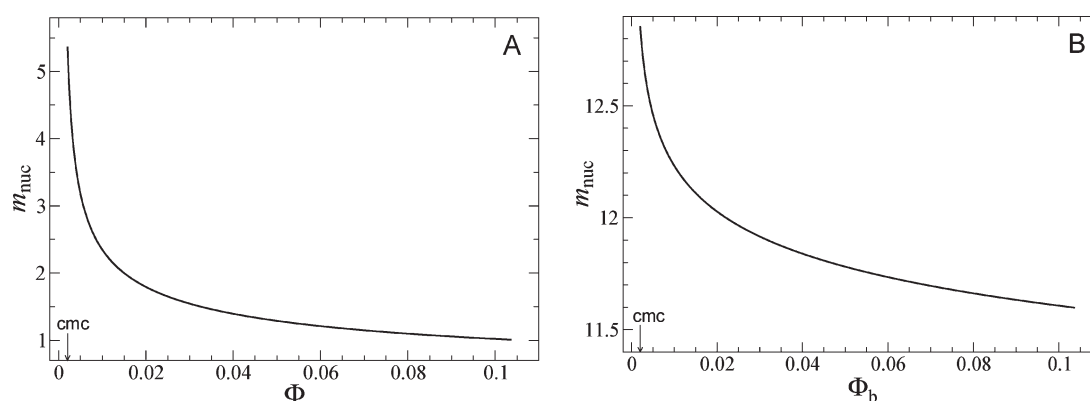

Figure 4. Critical nucleus size as a function of surfactant volume fraction in the range between $\varphi_3 = \varphi_{cmc} \simeq 2 \times 10^{-3}$ and φ_4 for closed (A) and open (B) systems. Parameters are given in Table 1.
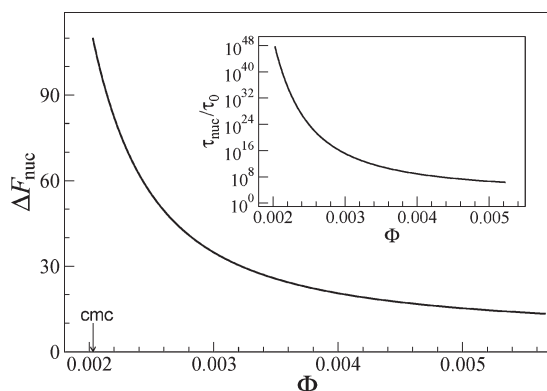

Figure 5. Nucleation barrier ΔF_{nuc} (in units of $k_B T$) as a function of surfactant volume fraction for a closed system. The inset shows the corresponding nucleation time (in units of the molecular time τ_0). Parameters are given in Table 1.

reservoir is either blocked or very slow. (If it is not, micellization in the system will be dominated by simple transport of micelles from the reservoir.) Thus, the starting point for the nucleation stage in this case is different from that of a closed system; it is still a monomeric state but with a lower volume fraction, $\Phi = \Phi_1$, where $\Phi_1 = \Phi_1^b < \Phi_b$. Nucleation is again assumed to be much slower than monomer diffusion. Hence, the monomer volume fraction remains fixed at $\Phi_1 = \Phi_1^b$. At the same time it should

minimize F for the given $m(t)$, which in turn determines the value of the third state variable, Φ. As the nuclei grow, the total volume fraction increases, and the system proceeds along the path that satisfies the constraints $\Phi_1 = \Phi_1^b$ and $\Phi_1^*[m(t), \Phi] = \Phi_1^b$.

The nucleation path ends at the state of critical nuclei, which is also different from the closed-system saddle point, because the total volume fraction has not reached the bulk value, $\Phi < \Phi_b$. This state is calculated using the following procedure for the open case. First, we calculate the monomer volume fraction in the reservoir according to the equilibrium condition

$$\Phi_1^b(\Phi_b) = \Phi_1^*[m^*(\Phi_b), \Phi_b] \tag{9}$$

Second, we equate this monomeric volume fraction with the one in our open system at the saddle point

$$\Phi_1^*[m_{nuc}(\Phi), \Phi] = \Phi_1^b(\Phi_b) \tag{10}$$

thus determining (via eqs 5 and 6) the total volume fraction in the system, Φ, and the critical nucleus, m_{nuc}, as functions of Φ_b. Third, we use these results to calculate Φ_{nuc}, c_{nuc}, and V_1 as functions of Φ_b

$$
\begin{aligned}
\Phi_{nuc}(\Phi_b) &= \Phi - \Phi_1^b \\
c_{nuc}(\Phi_b) &= \Phi_{nuc}/(na^3 m_{nuc}) \\
V_1(\Phi_b) &= c_{nuc}^{-1} = \frac{na^3 m_{nuc}}{\Phi - \Phi_1^b}
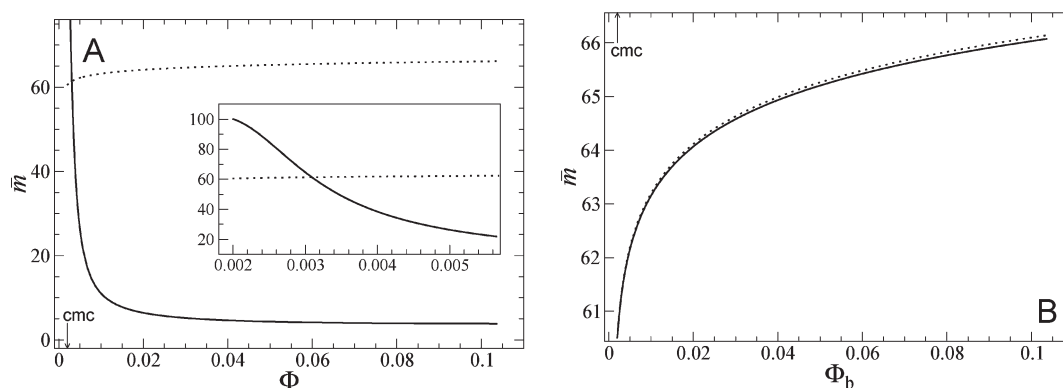\end{aligned} \tag{11}
$$

Figure 6. Intermediate micelle size at the end of the growth stage, $\bar{m}$, as a function of surfactant volume fraction in the range between $\varphi_3 = \varphi_{cmc} \simeq 2 \times 10^{-3}$ and φ_4 for closed (A) and open (B) systems. The inset in panel (A) focuses on volume fractions slightly above φ_3. Dotted lines show the equilibrium micelle size, m^*. Parameters are given in Table 1.
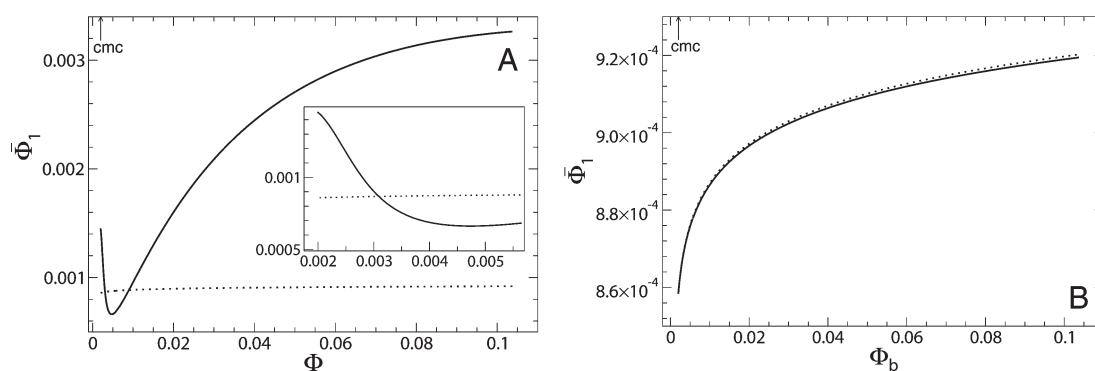

Figure 7. Intermediate monomer volume fraction at the end of the growth stage as a function of surfactant volume fraction in the range between $\varphi_3 = \varphi_{cmc} \simeq 2 \times 10^{-3}$ and φ_4 for closed (A) and open (B) systems. The inset in panel (A) focuses on volume fractions slightly above φ_3. Dotted lines show for comparison the equilibrium monomer volume fraction, Φ_1^*. Parameters are given in Table 1.

Finally, the nucleation barrier and time scale are given for the open system by

$$\Delta F_{\mathrm{nuc}}(\Phi_b) = \frac{V_1}{a^3}[F(\Phi, \Phi_1^b, m_{\mathrm{nuc}}) - F_1(\Phi_1^b)]$$
$$\tau_{\mathrm{nuc}}(\Phi_b) \simeq \tau_0 e^{\Delta F_{\mathrm{nuc}}(\Phi_b)} \tag{12}$$

From eqs 1–6 and 9–12, one can calculate the various parameters of the nucleation stage for an open system. Examples are shown in Figures 3B and 4B, revealing striking differences from the case of a closed system. The explanation is straightforward; the system is assumed to be in contact with the reservoir only through its monomeric concentration (so-called intermicellar concentration), Φ_1^b, which hardly changes as Φ_b is increased above the *cmc*. Hence, during this initial stage, Φ_1 remains low, regardless of the value of Φ_b. Consequently, the critical nuclei remain relatively rare and large, almost independent of concentration (Figures 3B and 4B). Moreover, since Φ_1 does not reach values above $\varphi_3 = \varphi_{cmc}$, we get very high nucleation barriers, resulting in an unphysical nucleation time for the open system. Thus, homogeneous nucleation in an open system, which does not have micellar transport from the reservoir, is strongly hindered. In the following discussion of open systems, it is assumed that, despite this strong kinetic limitation, nuclei were somehow caused to form.

MICELLAR GROWTH

The nucleation stage addressed in the preceding section ends when the critical nuclei have formed. On the free-energy landscape, the system has reached the saddle point of F. Subsequently, a stage of faster growth takes place. The free energy of the system decreases while the nuclei absorb additional monomers from the surrounding solution and m increases.

The growth is assumed to be much faster than the nucleation of new micelles or fusion and fission of existing ones. Hence, the concentration of micelles, $c_m = (\Phi - \Phi_1)/(na^3m)$ remains fixed at $c_m = c_{\mathrm{nuc}}$. Consequently, the available volume per aggregate, V_1, remains unchanged as well. We shall assume that the growth is also faster than the diffusive transport among the micelles (for closed and open systems) and with the reservoir (open system). The increase in m, therefore, comes solely at the expense of a decrease in the concentration of the surrounding monomers, while the total surfactant volume fraction is conserved. Thus, we describe the growth kinetics as a constrained path, $[\Phi_1(t), m(t)]$, such that $c_m = c_{\mathrm{nuc}} = \mathrm{const}$ and $\Phi = \mathrm{const}$.

Although diffusive transport into or out of the subsystem (of volume V_1) is assumed negligible during this stage, it is a priori unclear whether the growth process itself, within V_1, should be kinetically limited or diffusion-limited. We shall therefore examine both possibilities below. The constraints and the equations derived in this section apply to closed and open systems alike, yet
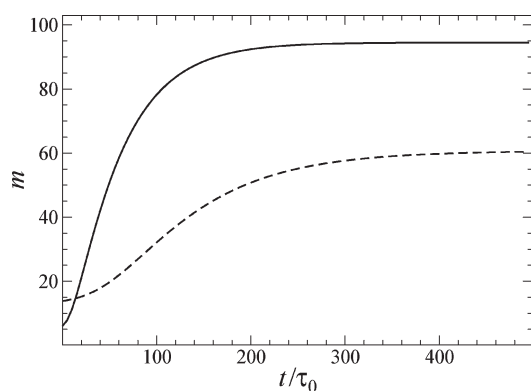
Figure 8. Temporal increase in micellar size assuming kinetically limited growth in closed (solid line) and open (dashed line) systems. The curves are obtained from numerical solution of eq 15 for the parameters given in Table 1, $\alpha = 1$, and $\Phi = 2.23 \times 10^{-3} = 1.1\varphi_3$ for the closed system, while for the open system, the same value is taken for Φ_b.

the values substituted for Φ and c_{nuc} differ substantially. While for a closed system Φ is the experimentally controlled surfactant volume fraction, for an open system, Φ gets the lower and weakly changing values determined from Φ_b in the nucleation stage according to eq 10. The concentration of nuclei is also much lower in the open-system case (cf. Figure 3). Consequently, the quantitative predictions for the two cases are quite different.

The aforementioned constraints imply that the average monomer volume fraction decreases linearly with the aggregation number, $m(t)$

$$\Phi_1(t) = \Phi - na^3 c_{nuc} m(t) \quad (13)$$

We are left with one independent variable, $m(t)$, whose change in time could be either kinetically controlled or diffusion-controlled. Yet, before studying the detailed evolution, let us examine its final state, which is common to both limits.

The final state of the growth stage, denoted as $(\bar{\Phi}_1, \bar{m})$, is given by the minimum of F along the constrained path, $(\partial F / \partial m)|_{c_m = c_{nuc}, \Phi = const} = 0$. This yields

$$m = \bar{m}: \quad \ln[\Phi_1(m)] + u(m) + mu'(m) + 1 - 1/m = 0 \quad (14)$$

where $\Phi_1(m)$ is given by eq 13 and, once $\bar{m}$ is calculated, $\bar{\Phi}_1 = \Phi_1(\bar{m})$. The resulting aggregation numbers and their dependence on the controlled surfactant volume fraction are presented in Figure 6. Note that the intermediate aggregation number at the end of the current stage is not equal to the equilibrium micellar size since it corresponds to a minimum of F along the constrained path rather than its global minimum. Unlike the equilibrium size, m^*, which is bound by thermodynamic stability to increase with surfactant volume fraction (dotted lines in Figure 6), the intermediate size $\bar{m}$ can have a richer behavior. Examined over a wider range of Φ, $\bar{m}$ is found to be nonmonotonous, having a maximum at $\Phi < \varphi_3 = \varphi_{cmc}$. Hence, for the closed system, it decreases with Φ (Figure 6A), whereas for the open system, which remains dilute throughout this stage, it increases with Φ (and, therefore, with Φ_b; Figure 6B). In the closed system, the growth overshoots the equilibrium size for $\Phi \gtrsim \varphi_3$ and undershoots it at higher values. Whether $\bar{m}$ is larger or smaller than m^* is in accord with the question of whether c_{nuc} is, respectively, smaller or larger than the equilibrium concentration of micelles. (We shall return to this point when we deal with the final relaxation.) In the open system, $\bar{m}$ is very close to, and slightly smaller than, m^*. Similar observations can be made concerning the intermediate monomer volume fraction, $\bar{\Phi}_1$, as demonstrated in Figure 7.

We now turn to the evolution of the micellar size. We shall first assume, in the first subsection below, that it is kinetically limited. We will subsequently check in the second subsection whether such a description is consistent with the rate of monomer diffusion and consider the alternative of a diffusive growth.

Kinetically Limited Growth. In the case of kinetically limited growth, the diffusive transport of molecules to the aggregate is assumed to be sufficiently fast so as not to limit the growth. The volume fraction of monomers, Φ_1, satisfies eq 13 while being uniform across the subsystem volume V_1. The increase of m with time is taken as proportional to the relevant thermodynamic driving force (i.e., the slope of F along the constrained path)

$$\frac{dm}{dt} = -\frac{\alpha}{\tau_0} \frac{V_1}{a^3} \frac{\delta F}{\delta m}\bigg|_{\substack{c_m = c_{nuc} \\ \Phi = const}}$$

$$= \frac{\alpha}{\tau_0} \{\ln[\Phi_1(m)] + u(m) + mu'(m) + 1 - 1/m\} \quad (15)$$

where α is an unknown dimensionless prefactor of order unity and $\Phi_1(m)$ is given by eq 13. Equation 15, supplemented by a proper initial condition for $m(t = 0)$, forms a simple initial value problem for the temporal increase in micelle size and is solved numerically. Because the initial state of this stage is a stationary (saddle) point of F, we cannot begin with the strict initial condition, $m(0) = m_{nuc}$, but have to perturb it to start the evolution. An example for a numerical solution of eq 15, where we have taken $m(0) = m_{nuc} + 1$ and $\Phi = 1.1\varphi_3 = 1.1\varphi_{cmc}$, is shown in Figure 8. The time scale of the growth, denoted as τ_k, is found to be about 2 orders of magnitude larger than the molecular time τ_0 (i.e., of order 10^{-6} s in this example).

To get an expression for the kinetic time scale, we examine the asymptotic behavior of eq 15 as m approaches $\bar{m}$, obtaining

$$|m(t) - \bar{m}| \approx e^{-t/\tau_k}$$

$$\tau_k^{-1} = \frac{\alpha}{\tau_0} \left[\frac{\Phi - \Phi_1}{m\Phi_1} - 2u'(m) - mu''(m) - 1/m^2 \right]_{m = \bar{m}, \Phi_1 = \bar{\Phi}_1}$$

$$(16)$$

The results for τ_k in terms of the molecular time τ_0 are shown in Figure 9. For the closed system, over one decade of surfactant volume fraction, τ_k decreases from $\sim 10^2 \tau_0$ to $\sim \tau_0$. (Values below τ_0, evidently, should not be regarded as physical.) The inset shows that the growth rate for the closed system increases roughly linearly with Φ. For the open system, the time scale is also about 2 orders of magnitude larger than τ_0, yet its dependence on Φ_b is much weaker for the reasons described in the Micellar Nucleation section.

Diffusion-Limited Growth. In the preceding subsection, we have assumed that the surrounding solution can supply the amount of monomers required for micellar growth within the time scale τ_k. Let us check whether this assumption is consistent with the rate of diffusive transport from the solution into the aggregate. The thickness of the diffusion layer around the aggregate, l_d (assumed to be much larger than the aggregate
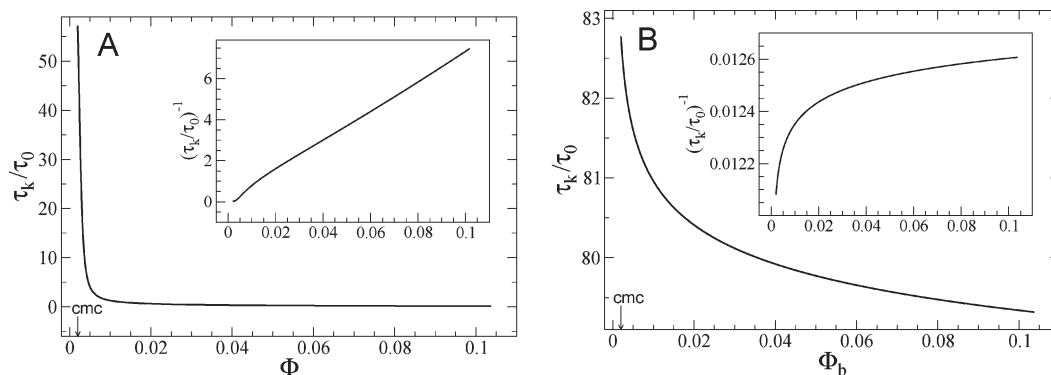
Figure 9. Time scale of kinetically limited growth as a function of surfactant volume fraction in the range between $\varphi_3 = \varphi_{cmc} \simeq 2 \times 10^{-3}$ and φ_4 for closed (A) and open (B) systems. The insets show the increase of τ_k^{-1} (growth rate) with Φ (in A) or Φ_b (in B). Parameters are given in Table 1, and we have set $\alpha = 1$ in eq 16.
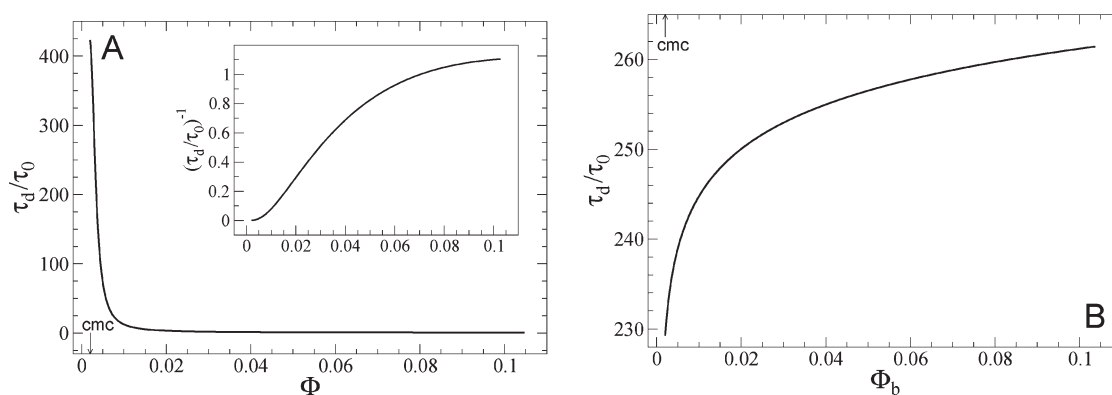

Figure 10. Time scale of diffusion-limited growth as a function of surfactant volume fraction in the range between $\varphi_3 = \varphi_{cmc} \simeq 2 \times 10^{-3}$ and φ_4 for closed (A) and open (B) systems. Parameters are given in Table 1.

radius), satisfies the equation $\Delta m = (4\pi/3)l_d^3 c_1$, where $\Delta m = \bar{m} - m_{nuc}$ is the number of monomers to be transported and $c_1 = \Phi_1/(na^3)$ is the monomer concentration. The diffusion time scale is then $\tau_d \approx l_d^2/D$, D being the diffusion coefficient of a monomer. Using the definition $\tau_0 \approx (na)^2/D$, we obtain

$$\tau_d/\tau_0 \simeq [3\Delta m/(4\pi n^2)]^{2/3}\Phi_1^{-2/3} \approx (0.1 - 1)\Phi_1^{-2/3} \quad (17)$$

where in the last relation, we have assumed $n \approx 10$ and $\Delta m \approx 50$. For our typical example of $\Phi_1 \approx 10^{-3}$ (cf. Figure 7), we get $\tau_d \approx (10-10^2)\tau_0$, that is, comparable to τ_k. Thus, the situation concerning the limiting process for micelle growth is not clear-cut, and both mechanisms may be relevant in general.

To treat the diffusion-limited growth in more detail, we employ the following approximations. First, we neglect the increase in the aggregate radius, R, and take it as constant. Although this description is evidently inaccurate, it crucially allows us to avoid the complicated treatment of a moving boundary. Since the growth does not begin from a single monomer but from a critical nucleus of finite size m_{nuc}, we do not expect the approximation of constant R to qualitatively affect the results. Second, the diffusion layer is assumed to be much smaller than the subsystem, $l_d \ll V_1^{1/3}$, thus allowing us to consider the latter as infinite and the monomer volume fraction far from the micelle, as given by eq 13. Third, we neglect desorption of monomers from the micelle to the solution during the growth. This is justified in view of the strong

driving force (large slope of F) for growth above the critical nucleus size.

We assume a radial volume fraction profile of monomers, $\Phi_1(r > R,t)$, which follows the diffusion equation

$$\frac{\partial \Phi_1}{\partial t} = D\frac{1}{r^2}\frac{\partial}{\partial r}\left(r^2\frac{\partial \Phi_1}{\partial r}\right) \quad (18)$$

The growth of a micelle is determined by the diffusive flux of monomers from the solution

$$\frac{dm}{dt} = D\frac{4\pi R^2}{na^3}\frac{\partial \Phi_1}{\partial r}\bigg|_{r=R} \quad (19)$$

The boundary condition far from the micelle is given according to eq 13 by

$$\Phi_1(r \rightarrow \infty, t) = \Phi - na^3 c_{nuc}m(t) \quad (20)$$

For the problem to be well-posed, eqs 18−20 should be supplemented by appropriate initial conditions for $\Phi_1(r,0)$ and $m(0)$, as well as a local "adsorption isotherm" at the aggregate surface, relating $\Phi_1(R,t)$ and $m(t)$. The latter lies beyond the scope of our coarse-grained description. At any rate, we are interested primarily in the qualitative asymptotics of the diffusive transport from the solution into the aggregate, for which these details are not crucial. The asymptotic behavior as the final state of the growth stage is approached is worked out in the Appendix,

yielding

$$\Phi_1(R, t \to \infty) \simeq \bar{\Phi}_1[1 - (\tau_d/t)^{3/2}]$$

$$\tau_d = \frac{a^2(n\Delta m)^{2/3}}{4\pi D}\bar{\Phi}_1^{-2/3} \qquad (21)$$

Thus, unlike the exponential relaxation of a kinetically limited process (eq 16), the diffusive relaxation is characterized, as usual, by a slow power law. Upon substituting $\tau_0 \approx (na)^2/D$ in eq 21, the general form of τ_d, derived earlier from heuristic arguments (eq 17), is confirmed.

Figure 10 shows the dependence of τ_d on the controlled surfactant volume fraction according to eq 21, where we have taken $\tau_0 = (na)^2/D$. The cases of closed and open systems are again found to behave qualitatively differently, τ_d strongly decreasing with Φ in the former and weakly increasing with Φ_b in the latter. This is a consequence of the different dependencies of $\bar{m}$ on concentration, commented on earlier (cf. Figure 6). In an open system, $\bar{m}$ increases with Φ_b [Figure 6B], and because more molecules are transported the longer the diffusive process takes (i.e., τ_d increases with Δm in eq 21), we get an increase of τ_d with Φ_b [Figure 10B]. Comparison of Figures 9 and 10 confirms our earlier assessment, that τ_k and τ_d are comparable in general, and both growth mechanisms may be relevant. Only for a closed system at concentrations slightly above the *cmc* do we get for our representative example $\tau_d \gg \tau_k$, that is, strictly diffusion-limited growth. (Note that τ_k and τ_d are associated with very different time dependencies — an exponential law vs a power law — and are defined only up to a numerical prefactor. Hence, they should be compared with respect to the order of magnitude only.)

Role of Bulk Diffusion. In the preceding subsection, we have considered the local diffusive transport that takes place around individual micelles, feeding them with monomers. In the case of an open system there should also be slower, long-distance diffusion of monomers from the bulk reservoir. In principle this should have been the next stage to consider. However, we find that the monomer volume fraction at the end of the growth stage, $\bar{\Phi}_1$, is invariably very close to the equilibrium (bulk) value, Φ_1^* (see Figure 7B). This is a consequence of the small number of initial nuclei (Figure 3B), whose growth consumes a small number of monomers. Thus, the driving force for bulk diffusion is very weak. Consistently, for the open system, we find also that the micellar size at the end of the growth stage, $\bar{m}$, is very close to the equilibrium size, m^* (Figure 6B). Therefore, the bulk diffusion that does occur in an open system has a very minor contribution to the micellization.

FINAL RELAXATION

At the end of the growth stage, monomer transport into the existing micelles has been exhausted, and the micelles have equilibrated with the surrounding monomers. Yet, the final state of this stage, $(\bar{\Phi}_1, \bar{m})$, does not correspond to the global free-energy minimum because up until now, we have constrained the concentration of micelles to remain at its nucleation value (cf. Figure 2). A slower process should ensue, therefore, during which the size and/or concentration of micelles relax to their equilibrium values.

In the open system, the situation is a bit unusual. (Recall from the Micellar Nucleation section, however, that actually reaching the current stage in an open system should already involve

overcoming unusually high barriers.) The monomer volume fraction has equilibrated with the bulk reservoir and reached its equilibrium value. The size of the existing individual micelles has equilibrated as well. What has not equilibrated yet is the total surfactant volume fraction, specifically, the contribution to Φ from Φ_m, the micellar volume fraction. Because there is no thermodynamic driving force for either monomer transport or changes in the size of the existing micelles and because we do not allow for transport of micelles from the reservoir, the only open pathway to final relaxation is the very slow nucleation of additional micelles. The newly formed micelles will take monomers from the solution, causing transport of additional monomers from the reservoir, until the total surfactant volume fraction reaches its equilibrium value, Φ_b.

The relaxation of the closed system is qualitatively different. Both the monomer volume fraction and aggregation number have not equilibrated yet and will change in time while keeping the total surfactant volume fraction fixed. Because there is no longer a driving force for directional exchange of monomers with the solution, we expect these changes to occur through fusion or fission of micelles. Such processes occur on the scale of an entire micelle and depend, therefore, on a different microscopic time, denoted τ_m. It is expected to be much larger than the molecular time τ_0, either because of the long diffusion time required for two micelles to meet before fusing (in which case, τ_m should be of order, say, $10^{-5} - 10^{-4}$ s) or due to kinetic barriers for fusion or fission. In addition, τ_m should depend on details of intermicellar interactions. Such kinetic barriers and interactions are not accounted for by the current model. Two additional processes, which in principle could be considered, are irrelevant in this case. First, nucleation of new micelles or complete disintegration of existing ones might occur but will require the much longer time scale of τ_{nuc} discussed earlier. Second, Ostwald ripening, a common relaxation mechanism in phase separation, where larger domains grow at the expense of smaller ones, is not expected to take place because the finite domains here (the micelles) are not unstable and the required positive feedback is thus lacking.

Either fission or fusion should be dominant, depending on whether $\bar{m}$ has overshot or undershot, respectively, the equilibrium size m^* (see Figure 6A). Correspondingly, the micellar concentration c_m will either increase or decrease with time. Over the time scale of these rearrangements of aggregate size and concentration, we can assume that the monomer volume fraction is relaxed, $\Phi_1(t) = \Phi_1^*[m(t), \Phi]$. We are left again with a single kinetic variable, either $m(t)$ or $c_m(t)$. The two are related via

$$c_m(t) = \{\Phi - \Phi_1^*[m(t), \Phi]\}/[na^3 m(t)] \qquad (22)$$

The kinetic equation for the micellar size reads

$$\frac{dm}{dt} = -\frac{\beta}{\tau_m}\frac{V_1}{a^3}f(m)$$

$$f(m) = \left.\frac{\delta F}{\delta m}\right|_{\substack{\Phi_1 = \Phi_1^*(m) \\ \Phi = \text{const}}} = \Phi_1^{*\prime}\ln\Phi_1^*$$

$$-\left[\frac{\Phi - \Phi_1^*}{m^2} + \frac{\Phi_1^{*\prime}}{m}\right]\ln(\Phi - \Phi_1^*) - (\Phi - \Phi_1^*)u'(m)$$

$$+ [u(m) + 1 - 1/m]\Phi_1^{*\prime} \qquad (23)$$

7276

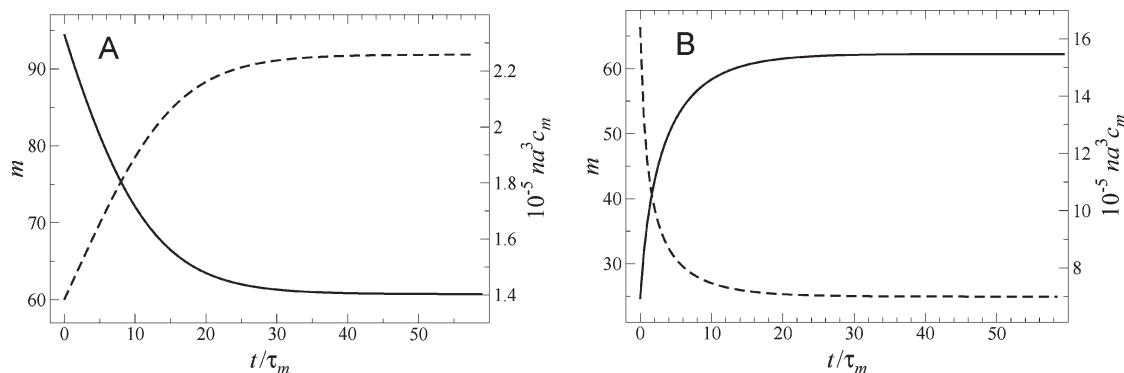dx.doi.org/10.1021/jp1073335 |J. Phys. Chem. B 2011, 115, 7268–7280

Figure 11. Evolution of micellar size (solid, left ordinate) and concentration (dashed, right ordinate) during the final relaxation stage in a closed system. Parameters are given in Table 1, we have set $\beta = 1$ in eq 23, and the volume fraction is $\Phi = 2.23 \times 10^{-3} = 1.1\varphi_3$ (A) and $5.23 \times 10^{-3} = 2.58\varphi_3$ (B).
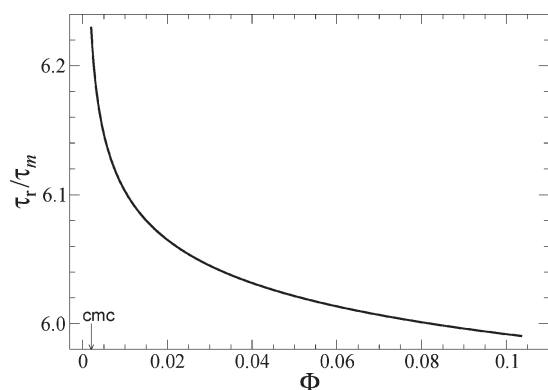

Figure 12. Time scale of final relaxation, τ_r (in units of the single-micelle time scale), as a function of the surfactant volume fraction in the range between $\varphi_3 = \varphi_{cmc} \simeq 2 \times 10^{-3}$ and φ_4 for a closed system. Parameters are given in Table 1, and we have set $\beta = 1$ in eq 24.

where $V_1 = na^3m^*/[\Phi - \Phi_1^*(m^*)]$ is here the volume per micelle at equilibrium, $\Phi_1^*(m)$ is given by eq 3, a prime denotes $\partial/\partial m$, and β is an unknown dimensionless prefactor of order unity.

Equations 3 and 23 are solved numerically to obtain $m(t)$ and, subsequently (via eq 22), also $c_m(t)$. Figure 11 shows the solutions for our exemplary surfactant and two volume fractions, corresponding to fission- and fusion-dominated relaxation.

To find the relaxation time, we examine the asymptotic behavior of $m(t \rightarrow \infty)$ according to eq 23, obtaining

$$|m(t) - m^*| \approx e^{-t/\tau_r}$$

$$\tau_r = \frac{\tau_m}{\beta} \frac{a^3}{V_1} \frac{1}{f'(m^*)} \qquad (24)$$

where $f(m)$ has been defined in eq 23. The dependence of τ_r on the surfactant volume fraction is shown in Figure 12. The relaxation time is found to weakly depend on Φ, remaining of the same order as (or slightly larger than) the single-micelle time τ_m throughout the concentration range.

■ DISCUSSION

The detailed picture which arises from our analysis of micellization kinetics is schematically summarized in Figures 13 and 14. We have divided the process of micelle formation into three major stages, nucleation, growth, and final relaxation. On the one hand, this crude separation into stages should be conceptually
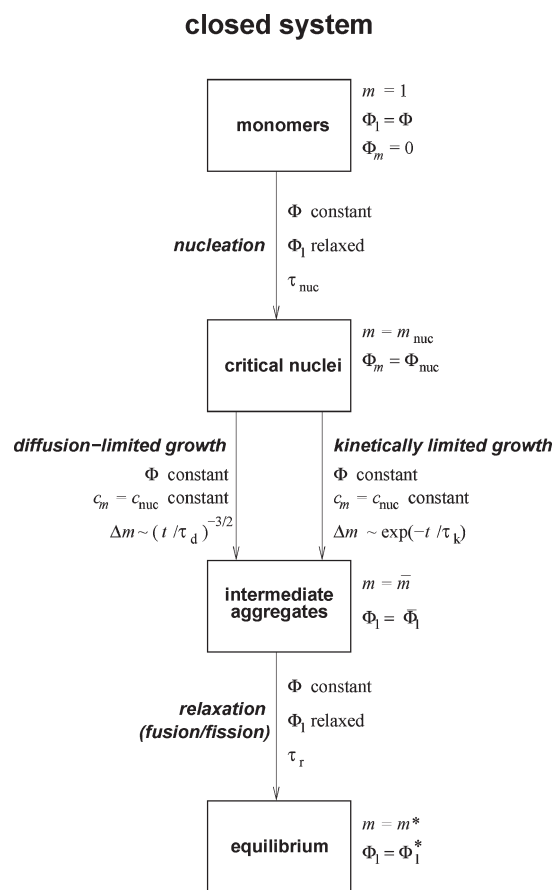

Figure 13. Schematic summary of micellization in a closed system. The states of the system are represented by rectangles, beside which the values of the state variables are indicated. The process is divided into three stages, represented by arrows. The constraints on the kinetics during each stage are indicated beside the arrows. (i) Slow nucleation stage (time scale τ_{nuc}), in which critical nuclei of size m_{nuc} form in a monomeric solution. (ii) Fast growth stage, in which the nuclei grow from m_{nuc} to an intermediate size $\bar{m}$ without changing their concentration. The growth may be either diffusion-limited (time scale τ_d with a $-3/2$ power law relaxation) or kinetically limited (time scale τ_k with an exponential relaxation). (iii) Final relaxation of the size and concentration of aggregates to their equilibrium values through fusion or fission (time scale τ_r).

valid because we find the corresponding time scales to be quite well separated. In particular, the nucleation time is found to be
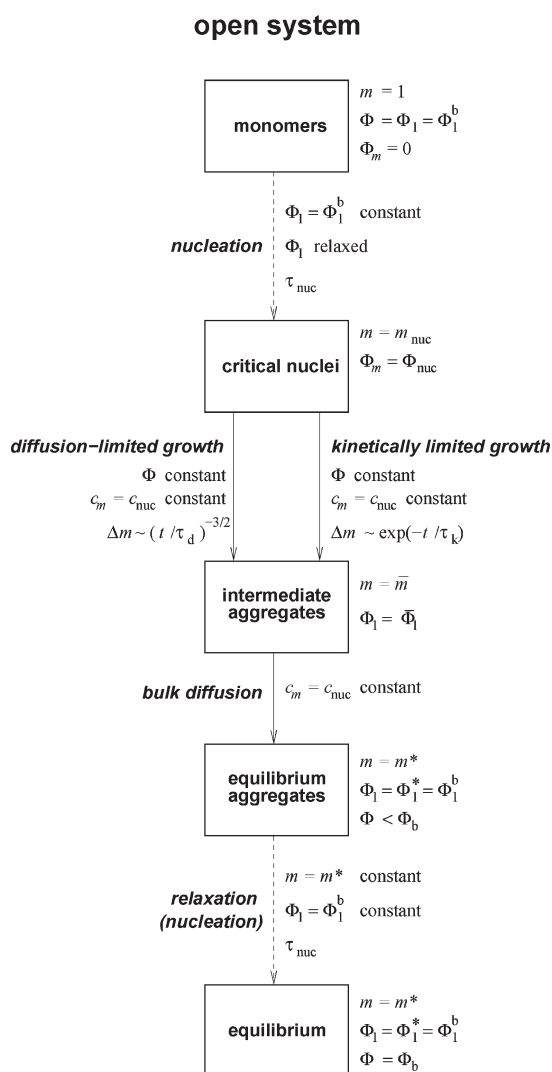
open system

Figure 14. Schematic summary of micellization in an open system, having monomer exchange with a reservoir. The states of the system are represented by rectangles, beside which the values of the state variables are indicated. The process is divided into four stages, represented by arrows. The constraints on the kinetics during each stage are indicated beside the arrows. (i) Slow nucleation stage (time scale τ_{nuc}), in which critical nuclei of size m_{nuc} form in a monomeric solution; this stage is found to be strongly hindered by kinetic barriers (dashed arrow). (ii) Fast growth stage, in which the nuclei grow from m_{nuc} to an intermediate size $\bar{m}$ without changing their concentration. The growth may be either diffusion-limited (time scale τ_d with a $-3/2$ power law relaxation) or kinetically limited (time scale τ_k with an exponential relaxation). (iii) Bulk diffusion from the reservoir until the aggregates reach their equilibrium size m^*; this stage is found to have a minor contribution to the micellization. (iv) Final relaxation of aggregate concentration through nucleation of additional micelles (also kinetically hindered; dashed arrow).

macroscopic, several orders of magnitude longer than the time scales of growth and equilibration. Such stages have been resolved in a recent X-ray scattering experiment on block copolymer micellization.[31] They also emerged in other micellization theories.[15] On the other hand, the discreteness of these stages, as illustrated in Figures 13 and 14, should not be taken too strictly. In particular, in the example treated above, we find the time scale of growth to be only 1–2 orders of magnitude shorter than the typical time for final equilibration. Thus, in certain cases,

it may well be that these two stages should not be considered as distinct.

The nucleation stage is much longer than all others, and because it is an activated process, its duration is exponentially sensitive to the surfactant volume fraction as well as other parameters (Figure 5). The range of nucleation times that we get for our exemplary surfactant in a closed system (typically larger than 1 s) is in line with measured values of $m\tau_2$, the time scale for formation or disintegration of entire micelles.[2] The high nucleation barriers found close to the equilibrium cmc ($\Phi = \varphi_3$) imply that the measured (apparent) cmc might, in certain cases, be higher than the equilibrium value. This issue, which was raised before in the context of block copolymer micelles,[13] clearly merits further study.

The growth stage occurs on much faster time scales (e.g., 10^{-6}–10^{-5} s for our example). These time scales are similar to those measured for τ_1, the single-monomer exchange time at equilibrium.[2] We have found that the growth may, in general, be either diffusion-limited or kinetically limited and that it should be diffusion-limited at concentrations close to the cmc. This is in accord with τ_1 being usually diffusion-limited for short-chain surfactants while becoming kinetically limited for longer-chain ones, which face higher kinetic barriers for incorporating into a micelle.[2] Our theory predicts a distinctive $-3/2$ power law relaxation in the case of diffusion-limited growth (eq 21). This prediction should be verifiable in scattering experiments like the one described in ref 31 when they are applied to short-chain surfactants.

The final relaxation stage in a closed system may involve either reduction in aggregate size (fission), accompanied by an increase in aggregate concentration, or the other way around (fusion) (see Figure 11.) Which of these scenarios holds depends on whether the aggregate size attained in the preceding growth stage has overshot or undershot the equilibrium aggregation number. The former should hold at concentrations close to the cmc, whereas the latter occurs at higher concentrations. We note that in the experiment of ref 31, the aggregates grew in size during their final relaxation, which is in line with the fact that the amphiphilic concentration in that experiment was much higher than its cmc. We note also that the somewhat surprising possibility of an intermediate aggregate size overshooting the equilibrium value was already pointed out in an earlier study.[27] An interesting consequence of our analysis is that, by tuning to the right surfactant concentration, one should be able to eliminate the final relaxation stage altogether, thus reaching the equilibrium micellar state already at the end of the fast growth stage. Another relevant prediction is that the relaxation time of this final stage should be almost independent of surfactant concentration (Figure 12). It should be stressed again that these predictions concerning the final relaxation stage require that the preceding growth stage be sufficiently fast so that the two processes could be considered separately. In particular, observing oversized micelles before they shed their extra molecules may be experimentally challenging.

Our findings concerning the kinetics of micelle formation have a number of additional experimental implications. A particularly clear-cut one relates to micellization in an open system, a solution in diffusive contact with a reservoir of monomers and micelles. We have found that in cases where only monomer exchange with the reservoir is allowed while the transport of micelles is blocked, micellization should be kinetically suppressed. The suppression is two-fold. First, strong activation is required for the homogeneous nucleation of the first micelles. This stems from the low surfactant concentration maintained in the system due to the

correspondingly low monomer concentration (sometimes referred to as the intermicellar concentration) in the reservoir. Second, even after micelles do nucleate and grow, the final relaxation of their concentration should be hindered because it requires the nucleation of additional micelles.

The consequential prediction is that the formation of micelles in such open monomeric solutions may be suppressed for a macroscopic time. In fact, this behavior is regularly manifest in applications involving micelle-enhanced ultrafiltration[39] and has been observed in dialysis experiments,[40] where the time scale of micelle formation was estimated to be 1−10 h. In both the ultrafiltration techniques and the dialysis experiment, a micellar solution is forced through a membrane whose pores are smaller than the micelles. The surfactant solution on the other side of the membrane remains monomeric for a macroscopic time, despite its contact with a micellar solution above the *cmc*. To our best knowledge, the analysis presented above provides the first quantitative account of this regularly observed behavior.

Apart from the aforementioned strong assumption of time scale separation, the main shortcoming of our model is its mean-field character. We have assumed that the kinetics in the surfactant solution can be described within a representative subvolume, V_1, containing a single aggregate and being uncorrelated with the other subvolumes. Upon closer inspection, in fact, we find that V_1 for a closed system typically contains $\sim 10-10^2$ surfactant molecules, which is comparable to the aggregation number. Hence, correlations among such subvolumes are to be expected as the micelles nucleate and grow. Another important mean-field aspect is our description of the state of the system as a deterministic point on the free-energy landscape and its kinetics as a sharply defined path on that landscape. In practice, and particularly close to the *cmc*, the system should be more accurately described by stochastic distributions, with polydispersity and occupancies of both the monomeric and aggregated states.[36] Nonetheless, we do not expect these approximations to qualitatively change the main results presented here.

■ APPENDIX

In this appendix, we calculate the asymptotic time dependence of the micellar size, $m(t)$, in a diffusion-limited growth. The equations to be handled are eqs 18−20.

To leading order at long times, we can substitute in eq 20 $m(t) \simeq \bar{m}$, turning the boundary condition far away from the micelle into $\Phi_1(r \to \infty, t) = \bar{\Phi}_1$. We now define $\psi(r,t) = \Phi_1(r,t) - \bar{\Phi}_1$, so that $\psi(r \to \infty, t) = 0$, and introduce Laplace-transformed variables, $\hat{\psi}(r,s) = \int_0^\infty dt \, e^{-st}\psi(r,t)$ and $\hat{m}(s) = \int_0^\infty dt \, e^{-st}m(t)$. The diffusion equation, eq 18, is then rewritten as

$$s\hat{\psi} = D\frac{1}{r^2}\frac{\partial}{\partial r}\left(r^2\frac{\partial\hat{\psi}}{\partial r}\right) \tag{A1}$$

where we have assumed $\psi(r,0) = 0$, as the accurate initial profile should not affect the long-time asymptotics. The boundary conditions, eqs 19 and 20, transform to

$$s\hat{m} - m_{\text{nuc}} = D\frac{4\pi R^2}{na^3}\frac{d\hat{\psi}}{dr}\bigg|_{r=R} \tag{A2}$$

$$\hat{\psi}(r \to \infty, t) = 0 \tag{A3}$$

The solution of eqs A1−A3 is

$$\hat{\psi}(r, s) = -\frac{na^3}{4\pi D}\left(\frac{s\hat{m} - m_{\text{nuc}}}{1 + R(s/D)^{1/2}}\right)\frac{e^{-(s/D)^{1/2}(r-R)}}{r} \tag{A4}$$

from which we get

$$\hat{\psi}(R, s) = -\frac{na^3}{4\pi DR}\left(\frac{s\hat{m} - m_{\text{nuc}}}{1 + R(s/D)^{1/2}}\right) \tag{A5}$$

The limit $t \to \infty$ corresponds to $s \to 0$, at which $s\hat{m} - m_{\text{nuc}} \simeq \bar{m} - m_{\text{nuc}} = \Delta m$. Inverting eq A5 back to real time and taking the limit $t \to \infty$, we find

$$\psi(R, t \to \infty) \simeq -\frac{na^3\Delta m}{8(\pi Dt)^{3/2}} \tag{A6}$$

which yields eq 21 for τ_d.

■ AUTHOR INFORMATION

Corresponding Author
*E-mail: hdiamant@tau.ac.il.

■ ACKNOWLEDGMENT

■ REFERENCES

(1) Israelachvili, J. *Intermolecular and Surface Forces*, 2nd ed.; Academic Press: London, 1992.

(2) *Dynamics of Surfactant Self-Assemblies*; Zana, R., Ed.; CRC Press: Boca Raton, FL, 2005.

(3) Aniansson, E. A. G.; Wall, S. N.; Almgren, M.; Hoffmann, H.; Kielmann, I.; Ulbricht, W.; Zana, R.; Lang, J.; Tondre, C. *J. Phys. Chem.* **1976**, *80*, 905–922.

(4) (a) Aniansson, E. A. G.; Wall, S. N. *J. Phys. Chem.* **1974**, *78*, 1024–1030. (b) Aniansson, E. A. G.; Wall, S. N. *J. Phys. Chem.* **1975**, *79*, 857–858.

(5) Almgren, M.; Aniansson, E. A. G.; Holmaker, K. *Chem. Phys.* **1977**, *19*, 1–16.

(6) (a) Lessner, E.; Teubner, M.; Kahlweit, M. *J. Phys. Chem.* **1981**, *85*, 1529–1536. (b) Lessner, E.; Teubner, M.; Kahlweit, M. *J. Phys. Chem.* **1981**, *85*, 3167–3175.

(7) Kahlweit, M.; Teubner, M. *Adv. Colloid Interface Sci.* **1980**, *13*, 1–64.

(8) (a) Hall, D. G. *J. Chem. Soc., Faraday Trans.2* **1981**, *77*, 1973–2006. (b) Hall, D. G. *J. Chem. Soc., Faraday Trans. 2* **1987**, *83*, 967–983.

(9) Wall, S.; Elvingson, C. *J. Phys. Chem.* **1985**, *89*, 2695–2705.

(10) Aniansson, E. A. G. *Prog. Colloid Polym. Sci.* **1985**, *70*, 2–5.

(11) De Maeyer, L.; Trachimow, C.; Kaatze, U. *J. Phys. Chem. B* **1998**, *102*, 8024–8028.

(12) (a) Kuni, F. M.; Grinin, A. P.; Shchekin, A. K.; Rusanov, A. I. *Colloid J.* **2001**, *63*, 197–204. (b) Kuni, F. M.; Grinin, A. P.; Shchekin, A. K.; Rusanov, A. I. *Colloid J.* **2001**, *63*, 723–730.

(13) Nyrkova, I. A.; Semenov, A. N. *Macromol. Theory Simul.* **2005**, *14*, 569–585.

(14) Ball, R.; Haymet, A. D. J. *Phys. Chem. Chem. Phys.* **2001**, *3*, 4753–4761.

(15) Neu, J. C.; Cañizo, J. A.; Bonilla, L. L. *Phys. Rev. E* **2002**, *66*, 061406.

(16) Smit, B.; Esselink, K.; Hilbers, P. A. J.; Van Os, N. M.; Rupert, L. A. M.; Szleifer, I. *Langmuir* **1993**, *9*, 9–11.

(17) von Gottberg, F.; Smith, K. A.; Hatton, T. A. *J. Chem. Phys.* **1998**, *108*, 2232–2244.

(18) Marrink, S. J.; Tieleman, D. P.; Mark, A. E. *J. Phys. Chem. B* **2000**, *104*, 12165–12173.

(19) Marrink, S. J.; de Vries, A. H.; Mark, A. E. *J. Phys. Chem. B* **2004**, *108*, 750–760.

(20) Mohan, G.; Kopelevich, D. I. *J. Chem. Phys.* **2008**, *128*, 044905.

(21) He, X.; Schmid, F. *Phys. Rev. Lett.* **2008**, *100*, 137802.

(22) Fujiwara, S.; Itoh, T.; Hashimoto, M.; Horiuchi, R. *J. Chem. Phys.* **2009**, *130*, 144901.

(23) de Moraes, J. N. B.; Figueiredo, W. *Chem. Phys. Lett.* **2010**, *491*, 39–43.

(24) Halperin, A.; Alexander, S. *Macromolecules* **1989**, *22*, 2403–2412.

(25) Haliloglu, T.; Bahar, I.; Erman, B.; Mattice, W. L. *Macromolecules* **1996**, *29*, 4764–4771.

(26) Dormidontova, E. E. *Macromolecules* **1999**, *32*, 7630–7644.

(27) Besseling, N. A. M.; Cohen Stuart, M. A. *J. Chem. Phys.* **1999**, *110*, 5432–5436.

(28) Zana, R.; Marques, C.; Johner, A. *Adv. Colloid Interface Sci.* **2006**, *123−126*, 345–351.

(29) (a) Lund, R.; Willner, L.; Stellbrink, J.; Lindner, P.; Richter, D. *Phys. Rev. Lett.* **2006**, *96*, 068302. (b) Lund, R.; Willner, L.; Stellbrink, J.; Lindner, P.; Richter, D. *Phys. Rev. Lett.* **2010**, *104*, 049902.

(30) Lund, R.; Willner, L.; Richter, D. *Macromolecules* **2006**, *39*, 4566–4575.

(31) Lund, R.; Willner, L.; Monkenbusch, M.; Panine, P.; Narayanan, T.; Colmenero, J.; Richter, D. *Phys. Rev. Lett.* **2009**, *102*, 188301.

(32) Choi, S.-H.; Lodge, T. P.; Bates, F. S. *Phys. Rev. Lett.* **2010**, *104*, 047802.

(33) Diamant, H.; Andelman, D. *J. Phys. Chem.* **1996**, *100*, 13732–13742.

(34) Diamant, H.; Ariel, G.; Andelman, D. *Colloids Surf., A* **2001**, *183−185*, 259–276.

(35) Ariel, G.; Diamant, H.; Andelman, D. *Langmuir* **1999**, *15*, 3574–3581.

(36) Hadgiivanova, R.; Diamant, H. *J. Phys. Chem. B* **2007**, *111*, 8854–8859.

(37) Hadgiivanova, R.; Diamant, H. *J. Chem. Phys.* **2009**, *130*, 114901.

(38) Maibaum, L.; Dinner, A. R.; Chandler, D. *J. Phys. Chem. B* **2004**, *108*, 6778–6781.

(39) Pramauro, E.; Bianco Prevot, A. Detergent Formulations in Separation Science. In *Handbook of Detergents, Vol. 128, Part D: Formulation*; Showell, M. S., Ed.; CRC Press: Boca Raton, FL, 2006; Chapter 10, pp 305−323.

(40) Morigaki, K.; Walde, P.; Misran, M.; Robinson, B. H. *Colloids Surf., A* **2003**, *213*, 37–44.